Detection of Parkinson's Disease on DaTSCAN Image Using Multi-kernel Support Vector Machine

Kavitha Paranjothi[1]*   Fathima Ghouse[2]   Revathi Vaithiyanathan[3]

[1]*Department of Computer Science and Engineering, CMR Institute of Technology, Bengaluru, India*
[2]*Department of Computer Science and Engineering, Adhiyamaan College of Engineering, Hosur, India*
[3]*Department of Computer Science and Engineering, Dayananda Sagar University, Bengaluru, India*
* Corresponding author's Email: kavitha.p@cmrit.ac.in

Abstract: Parkinson's disease (PD) is a degenerative illness of central nervous system primarily caused by neuronal degeneration in substantia nigra of the brain. A biomarker for Parkinson's disease (PD) is represented by blood uric acid level. Although, the relationship between Parkinson's disease, and diabetes and the outcome of specific treatments remains unclear. Quantitative analysis of the images can increase the potential of dopamine transporter (DAT) and single-photon emission computed tomography (SPECT) images as a biomarker for tracking PD progression. To predict Parkinson's disease using DaTscan images, an ensemble of Machine Learning (ML) models was developed. In this work, Parkinson's Progressive Markers Initiative (PPMI) datasets were utilized for collecting the data on PD. Initially, feature extraction was done using the VGG-16, and AlexNet to classify Parkinson's illness. In following stage, a predicted classification of Parkinson's cases and healthy controls is generated using the Multi-kernel Support Vector Machine (MSVM) model to enhance overall final output of classification model. PPMI has made a database that is accessible to individuals for use in evaluating the proposed model. Compared with existing methods of Explainable Boosting Machine (EBM), Light Gradient Boosting Machines (LGBM) & Random Forests (RF), Convolutional Neural Network (CNN), Bayesian CNNs, CNN with Fuzzy Rank Level Fusion (CNN+FRLF), and EfficientNet-B0 and MobileNet-V2 models the implemented MSVM achieves high accuracy. When compared with the existing methods the implemented MSVM method obtained 98.60% of accuracy.

Keywords: DaTscan image, Machine learning, Parkinson's disease, Parkinson's progression markers initiative (PPMI).

1. Introduction

PD which affects a significant portion of the older population, is second most prevalent neurological illness after Alzheimer's disease (AD) [1]. The underlying cause of PD is thought to be degenerating of dopaminergic neurons in substantia nigra, that manifests as motor symptoms such as tremors, akinesia, trouble speaking, pain, and irregular walking [2]. The most often utilized diagnostic method for determining the dopamine deficit in PD is SPECT using DaTSCAN (123I-Iofupane) [3]. The term "neurodegenerative" describes a condition in which the brain cells eventually die. ML which has easy integration and excellent accuracy, is being utilized more often to identify medical disorders [4]. Additionally, employed an ML-based method that incorporates a linear Support Vector Machine (SVM), and k-nearest neighbors (K-NN) classifier to determine level of movement in Parkinson's patients [5]. This research established a framework for PD-generating prediction in time-series data because of its ability to describe the expected result [6]. The main structure of classification systems used in CAD tools is as follows: (i) delineating the areas of interest (ROI) to concentrate the analysis on them, (ii) extracting the features from these regions, and (iii) classifying the data based on those characteristics. Deep neural networks are trained to create a customized feature space for the best class separation,

46

in contrast to traditional approaches that extract predetermined features [7].

Whereas machine-earning techniques are excellent at processing straightforward linear data, they challenge complex medical data [8]. The transition from manual healthcare diagnosis to efficient CAD-based systems could facilitate a substantial expansion of healthcare system by expanding diagnosis, preventing false diagnosis, and consequently reducing death rates [9]. There is an increasing interest in the automated classification of the brain in medical imaging to aid in the identification of neurological and mental disorders through ML approaches [10]. Finding the characteristics that the CNN automatically learns during the training phase is challenging due to the multilayer nonlinear nature of the CNN [11]. Early-stage dopamine transporter imaging with 123I-Iofupane shows a high degree of predictive specificity for medically undetermined PD, Parkinsonian syndromes (PS), and dementia with Lewy bodies (DLB) [12]. The initial source of SPECT images, which were pre-processed using data normalization techniques and scaled between 0 and 1, originated from the PPMI dataset [13]. The ability to effectively categorize and forecast many brain diseases has been demonstrated by machine learning-based CAD systems that make use of picturing data and electronic medical records [14]. The study's primary contributions are as follows;

- The establishment of an effective machine learning algorithm for the DaTscan-based initial recognition of Parkinson's disease.
- The PPMI dataset for PD classification was utilized for model training and testing to assess the robustness and effectiveness of the brain illness system in real-time.
- The VGG-16 and AlexNet CNN models are used for feature extraction performance as they relate to this medical imaging task.

The research paper is given as follows; the literature survey of the related work was detailed in Section 2. The implemented method is described in Section 3. Experimental result was explained in Section 4. Finally, conclusion of this research is discussed in Section 5.

2. Literature survey

Sarica [15] implemented the Explainable Boosting Machine (EBM), a new ML glass-box model based on Generalized Additive Models plus interactions (GZ^2MS), which was used to provide explainable in categorizing SWEDD and PD while maintaining optimal performance. The EBM improves the basic GA2 Ms by gradient and bagging increases with tree-like shallow ensembles to lessen co-linearity and avoid overfitting. However, this method had poor specificity in identifying PD class, and had large training process.

Junaid [16] implemented an RF and LGBM of ML approaches for PD progression prediction based on time-series data. The implemented method objective was to create a reliable and comprehensible ML pathway for the prediction of PD progression. This model's performance improved dramatically when feature selection with optimization was used instead of all features and the model was run faster. Due to insufficient sample sizes, this method had flaws in PD validation test results.

Arco [17] implemented a Bayesian CNNs, multi-level ensemble classification system using a Bayesian Deep Learning technique to increase efficiency by presenting the uncertainty of each categorization result. In this system, a prediction with less uncertainty was given more weight than one with higher uncertainty during the decision-making process. However, this implemented method had less identification patterns performance in various PD illness.

Nazari [18] implemented a Convolutional Neural Network (CNN) that was used to classify SPECT images of dopamine transporter accessibility in Parkinsonian syndrome patients and address clinical uncertainties. LRP's resilience was increased by reducing relevance spill-out and preventing noise amplification caused by the gradient shattering effect. However, this implemented CNN method had misclassification in DAT-SPECT of visual interpretation.

Nakajima [19] implemented 123-Iofupane images from patients of 239 with questionable neurodegeneration illnesses or mental illnesses and categorized them as non-PS/PD/DLB or PS/PD/DLB. For training, 137 images from one hospital were examined for image attributes of high or low uptake (F1), symmetry (F2), dot- or comma-like caudate patterns, and uptake putamen (F3). The model multivariate with three characteristics and age had the greatest diagnosis accuracy for distinguishing PS/PD/DLB when compared to the traditional ROI-based approach. However, this method had less accuracy performance in PD image professional classifiers.

Alsharabi [20] implemented an AlexNet-quantum transfer learning method to analyze neurodegenerative disease using a magnetic resonance imaging (MRI) dataset. Through the use of a traditional pre-trained AlexNet model and a quantum variational circuit (QVC), the hybrid model

was created by generating a predictive vector of features from high-dimensional data. The AlexNet-quantum transfer learning technique has increased the model's performance while also increasing its speed and classification accuracy automatically. Due to large training process time, this method had affected the model's efficiency.

Zhou [21] implemented a mixture of linear dynamical systems (MLDS) models for measuring varying PD progression utilizing DaTSCAN images. This model assigns PD cases to several progression subtypes, with every subtype characterized by a linear dynamical system (LDS) multivariate. Reduction in asymmetry has the quickest feasible interval time among all LP, RP, RC, and LC, according to MLDS of linear combinations. However, this method had less PD classification utilized by DaTscans images.

Ankit Kurmi [22] implemented Convolutional Neural Network with Fuzzy Rank Level Fusion (CNN+FRLF) method utilized for PD detection UTILIZING DaTscan images. This implemented ensemble approach for the detection of PD that integrates decision scores obtained from four different DL models. The implemented method used GUI-based software tool had performed and effectively detected the PD disease in real-time. However, this implemented method high misclassification, hence to decreased number of inaccurate classifications and to test FRLF ensemble technique on other datasets.

Hajer Khachnaoui [23] implemented EfficientNet-B0 and MobileNet-V2 models based on CNN which were utilized for enhanced Parkinson's disease diagnosis. This method specifically employed Bilinear CNN (BCNN) for PD diagnosis, which represented a novel application of this technique. The BCNN was combined with pre-trained CNN models obtained increased classification of Parkinson's disease. Due to relatively small dataset, this method had restricted the generalizability of PD categorization.

From this section, a professional image classifier requires information to increase its precision. Large datasets and shorter training times have an impact on model performance. Extra-striatal areas affected by PD are not accounted for in the model. These are some of the overall limitations mentioned in the related papers. So, the MSVM is implemented to overcome these drawbacks in the detection of PD on DaTSCAN Images.

3. Methodology

The implemented model's architecture is described in this section for detecting Parkinson's disease effectively. The work involves the PPMI dataset, pre-processing using normalization, VGG-16, and AlexNet is used for feature extraction, Improved Marine Predictor Algorithm (IMPA) utilized for feature selection, and MSVM is employed for the image classification process. Fig. 1 illustrates the block diagram of implemented model. The SPECT images from the PPMI dataset were used to train the implemented model. A memory set is also taken into consideration during training to increase robustness and minimize overfitting.

3.1 Dataset

Information used in this study was attained from the database of the Parkinson's Progressive Markers Initiative (PPMI). The Dataset consists of 642 DaTscans SPECT images split into non-PD (N = 212) and PD (N = 430) groups. There were no subsequent scans of the same point; the data utilized was only from distinct patients' initial screening. This was done to maintain the dataset's originality and to enhance the study's goal of early detection. Another purpose was to avoid over-fitting, which could be brought on by scans from the same patient being too similar to one another during model training.
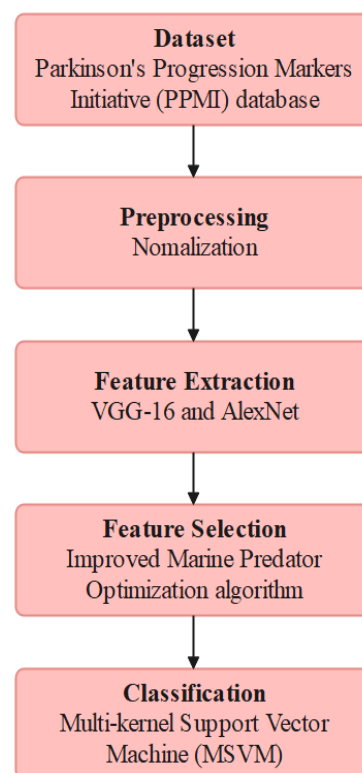

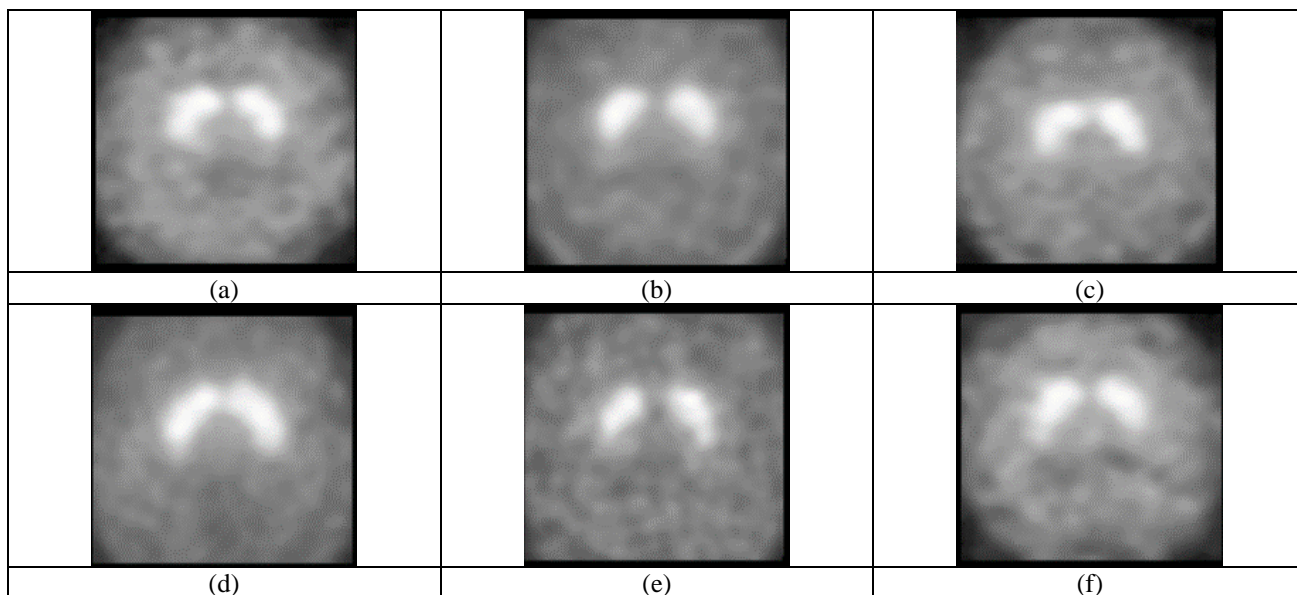Figure. 1 The block diagram of the implemented method

Figure. 2 PPMI dataset for a person suffering from PD

Table 1. Patient Demographics

Category	Healthy Control	Parkinson's Disease
Number of patients	212	430
Sex (Female)	84	152
Sex (Male)	128	278
Age (Maximum)	84	85
Age (Minimum)	31	33

To preserve the validity of the dataset, scans without evidence of dopaminergic deficiency (SWEDD) individuals were also eliminated. Table 1 lists the demographics of the patient's information that was collected and Fig. 2. represents the sample images of the PPMI dataset for a person suffering from PD.

3.2 Pre-processing

Normalization was utilized as a pre-processing technique to ensure that the deep learning model maintained its high degree of performance generalization even after multiple training iterations. Learning the visual characteristics in the same brain of many modes while gaining adaptation is beneficial. In the computer vision field, recognition of patterns, and other domains, normalization of images is a broadly utilized approach. This work utilized z-score normalization. It's expressed in Eq. (1):

$$z = \frac{x - \mu}{\sigma} \quad (1)$$

Where μ denotes the value of mean, and σ denotes standard deviation.

Following that, MRI image (240, 240, 155) is then arbitrarily chopped into a matrix (144, 144, 128) using a method of random 3D clipping. Reduced image is rotated by angle U (10, +10) using a random 3D rotation technique. Random intensity enhanced method for 3D images is used to set the value of each image pixel as follows in Eq. (2):

$$x_{new} = x_{old} * U (0.9, 1.1) + U(-0.1,\ 0.1) \quad (2)$$

Where, U denotes uniform distribution. Image is symmetrically arranged in the breath, height, and depth dimensions because of random mirror processing. Employing several image-enhancing methods to increase the size of the training dataset, can enhance the performance and generalizability of deep neural networks. Then, pre-processed input image is given to the feature extraction step as input.

3.3 Feature extraction

This section provides a technical summary of the AlexNet and VGG-16 models. Given that FC-8 is the final fully connected layer in these two topologies, the RFE method was applied to the characteristics attained from these layers. One of the most prominent CNN architectures is the AlexNet. Layers that are convolutional, pooling, and fully connected make up this architecture. 227x227 pixels make up the input size, it is based on a method where 5x5 and 3x3 pixel filters are moved over the image in the convolutional layer. To move the following layer, activation maps with more efficient characteristics are produced. The most important feature of activation maps is their significant characteristic. Without affecting the

image's features, the pooling layer is employed to minimize the image's cost and size.

The architecture of VGG-16 has FC layers, pooling, and convolutional, similar to AlexNet. It consists of 21 layers in total, and this architecture is characterized by a developing network structure. The input is 224x224 pixels in size, and the convolutional layer's filter has a 3x3 pixel filter size. The last layer in this architecture has a completely connected layer that was utilized for the extraction of features.

For feature extraction in this work, architectures of CNN are utilized. Every FC-8 layer in the model contained 1000 deep features. Both models have a filter size of 3x3 pixels, several strides are set to 2, and the docking type is set to maximum. The dataset was divided into two classes based on rates: 30% for testing and 70% for training.

3.4 Feature selection

An essential step in machine learning algorithms is feature selection, which finds unique related subsets of features. The method improves prediction accuracy and information understanding. The huge search space makes it difficult to evaluate feature selection vectors with N variant combinations directly. Perfect feature selection difficulties can be solved by metaheuristic algorithms like IMPA. To find the best feature subset, IMPA searches the feature space and chooses the most important and best features. With the fewest possible selected features, the ideal approach maximizes classification accuracy and reduces the mistake rate. A total number of 8192 outputs were extracted from feature extraction, which contains 4096 from VGG-16 and 4096 from AlexNet. The input for feature selection is the extracted outputs.

3.4.1. Improved marine predictor algorithm

An updated marine predator algorithm called IMPA is implemented to address the MPA's current drawbacks. IMPA enhances MPA by combining a quasi-opposition learning technique and concept of differential evolution. First, increasing population variety and accelerating MPA convergence are achieved by employing a quasi-opposition learning technique. The basic goal of differential evolution is to make MPA more adept at escaping local optimal, and it offers operation of crossover, mutation, and selection to that end. Accurate implementation of enhanced algorithm is given below.

3.4.1.1 Quasi-opposition learning strategy

A quasi-opposition learning technique (QOL) has been described, based on the principles of opposition-based learning (OBL). It can increase algorithm performance, faster convergence and increase population variety. By determining the opposing solution to the existing solution in search space, OBL broadens search space. Following is the opposition solution of specific calculation in Eq. (3),

$$X_i' = lb + ub - X_i \qquad (3)$$

where the current solution is denoted as X_i, the search agent of lower and upper bounds is denoted as lb and ub.

In the computation for quasi-opposition learning, quasi-opposition point lies halfway between opposition point and the midpoint. This indicates that the quasi-opposition point is more likely to be ½ as close to the unknown optimal solution as the current solution and that it is closer to the ideal solution, which may accelerate convergence. Quasi-opposition point is calculated using the following Eq. (4),

$$X_i^q = \begin{cases} m + (m - X_i) \times r_1, & if \ X_i < m \\ m - (X_i - m) \times r_2, & else \end{cases} \quad (4)$$

where uniform random number in [0,1] denoted r_1 and r_2, and midpoint of current search space is denoted $m = \frac{lb+ub}{2}$.

The quasi-opposition solution is calculated for each person using the quasi-opposition learning approach, and current solution of fitness values and quasi-opposition solution are then determined. Present population was selected by first sorting the individuals with the highest fitness values into ascending order, and then using that population to explore and exploit the MPA process. To classify Parkinson's disease, the features produced by the feature extraction procedure are passed on to the phase of feature selection.

3.5 Classification of the MSVM model

Multi-kernel Support Vector Machine (MSVM) classification

To predict a certain data input, the class label, for example, predictive modeling is used to solve classification issues in machine learning. To generate multi-kernel SVMs, typically many two-class SVMs are concatenated. Kernel can take information as is and transform it into required structure. Different types of piece functions are used in distinctive SVM classifications. These activities might take many

50

different forms. Radial Base Function (RBF), sigmoid, polynomial, linear, and nonlinear functions are employed in MSVM.

3.5.1. Linear kernel SVM

It is used for data can be divided into 2 groups utilizing simply a single straight line, which is known as data that can be separated linearly. To boost its generalization capability, it seeks to broaden this margin as much as possible. According to Eq. (5), linear function is dot product of the two vectors z1 and z2.

$$Y(Z1, z2) = z1.z2 \qquad (5)$$

3.5.2. RBF SVM

For many nonlinear problems, the Gaussian kernel provides separation of good linear in larger dimensions. The variable that is subject to change Sigma has a big impact on how effective kernel is and can be changed depending on the specific problem. It responds almost linearly when the exponential is overestimated, losing higher-dimensional projection's non-linear strength. Decision boundary will particularly susceptible to noise in data of training if feature is devalued, on the other hand, as this will result in a lack of regularisation. The distance from the origin or a particular location affects the function's value. Where $\alpha = 1/2\sigma^2$ & $\alpha > 0$ in Eq. (6),

$$Y(z1, z2) = exp(-\alpha\|z1 - z2\|^2) \qquad (6)$$

3.5.3. Sigmoid SVM

The function of tanh is utilized in this kernel. This can be utilized as an alternative for the neural network given in Eq. (7). Where the slope is α and the intercept constant is d. α is 1/N for a common value, here N is denoted as data dimension. An artificial neuron activation function is utilized that is equivalent to a 2-layer perceptron neural network model.

$$Y(z1, z2) = \tanh(\alpha.z1^T.z2 + d) \qquad (7)$$

3.5.4. Polynomial kernel SVM

It's a representation of a linear kernel that is more essentially structured. Eq. (8) represented the polynomial kernel. Where the polynomial degree is

denoted as e and the z1 & z2 are the vectors in the given Eq. (8),

$$Y(z1, z2) = (z1.z2 + 1) * e \qquad (8)$$

Using the Multi-kernel Support Vector Machine enhances the accuracy and performance of Parkinson's disease detection. Thus, the classification is performed utilizing most significant and pertinent features. Further, results are shown in section 4.

4. Experimental result

The implemented improved model is simulated in this research utilizing the MATLAB (2018a) environment with following system requirements: operating system as Windows 10 (64 bit), 16 GB of RAM, and an Intel Core i7 process. The model was tested utilizing an image sequence X_v, with N = 64 (PD = 42, non-PD = 21) and employing a sequence of images to train X_t, M = 156 (PD = 346, non-PD = 170), respectively. X_t and X_v are expressed in below Eqs. (9) and (10).

$$X_t = \left\{x_t^{(1)}, x_t^{(2)}, \ldots, x_t^{(M)}\right\} \qquad (9)$$

$$X_v = \left\{x_v^{(1)}, x_v^{(2)}, \ldots, x_v^{(N)}\right\} \qquad (10)$$

The relevant class label sequences Y_t and Y_v were employed in these sets are expressed in below Eqs. (11) and (12)

$$Y_t = \left\{Y_t^{(1)}, Y_t^{(2)}, \ldots, Y_t^{(M)}\right\} \qquad (11)$$

$$Y_v = \left\{Y_v^{(1)}, Y_v^{(2)}, \ldots, Y_v^{(N)}\right\} \qquad (12)$$

To effectually reduce cross-entropy using loss function and fit distribution p(y) in Eq. (13),

$$LE = -\frac{1}{N}\sum_{i=1}^{N}\log(p(y_i)) \qquad (13)$$

Where, number of instances is denoted as N, in y_i classes are shown in either (y_0) of negative classes or (y_1) of positive classes. From a mathematical respective Eqs. (14) and (15),

$$y_i = 1 \implies \log(p(y_i)) \qquad (14)$$

$$y_i = 0 \implies \log(1 - p(y_i)) \qquad (15)$$

As a result, the loss function of binary cross-

entropy is given by the following Eq. (16),

$$LE = -\frac{1}{N}\sum_{i=1}^{N} y_i.\log(p(y_i))$$
$$+ (1-y_i).\log(1-p(y_i)) \quad (16)$$

Through a 16 validation batch size and a training batch size of 32, training images received spontaneous argumentations along the Image Data Generator class. Training a step size of 32 was used throughout the model's 300 epochs of training. The basic rule of thumb was used to determine the step size, which is to multiply the result of dividing, the quantity in the dataset separated by batch size by a positive value larger than one, often to explain argumentations. The step size of validation was determined similarly and started to be 4 steps. The learning rate was initially set to 103 and Adam optimizer was the name of the optimizer that was in use from the library of Kera's optimizers. For the first instant (beta 1), the exponential decay rate value was 0.9, and for the moment of a second (beta 2), its value was 0.999. The exponential decay rate needs to be near 1.0 for issues that are indicated by a gradient sparse, such as computer vision. A cloud-based Tensor Processing Unit (TPU) device needed 5460 seconds, or about 1.5 hours, to complete training procedure. The performances are evaluated using the below-mentioned Eqs. (17) -(23),

$$Specificity = \frac{No.of\ true\ Negatives}{No.of\ True\ Negatives+No.of\ False\ Positives} \times 100 \quad (17)$$

$$Sensitivity = \frac{No.of\ True\ Positives}{No.of\ True\ Positives+No.of\ False\ Negatives} \times 100 \quad (18)$$

$$Precision = \frac{No.of\ True\ Positives}{No.of\ true\ Positives+No.of\ False\ Positives} \quad (19)$$

$$Accuracy = \frac{True\ Positive+True\ Negative}{True\ positive+True\ Negative+False\ Positive+False\ Negative} \times 100 \quad (20)$$

$$MCC = \frac{TP\times TN-FP\times FN}{\sqrt{(TP+FP)(TP+FN)(TN+FP)(TN+FN)}} \times 10 \quad (21)$$

$$F-score = \frac{2TP}{2TP+FP+FN} \times 100 \quad (22)$$

$$Recall = \frac{TP}{TP+FN} \quad (23)$$

4.1 Quantitative analysis

Tables 2-4 show improved performance analysis in terms of precision, sensitivity, specificity, accuracy, and MCC real and optimized feature selection without the need for augmentation. Table 2. Represents simulation outcomes of MSVM by different classifiers for PPMI dataset. Figs. 3 and 4 represent quantitative analysis of several classifiers' actual and optimized feature selection for the dataset of PPMI.

In comparison to classifiers optimized feature selection, those on PPMI dataset had highest performance metrics. Results of MSVM, simulations employing PPMI database with various classifiers are shown in Table 2. Implemented MSVM is compared to DNN (Deep Neural Network), NN (Neural Network), RNN (Recurrent Neural Network), and GAN (Generative Adversarial Network) in terms of precision, accuracy, sensitivity, specificity, and MCC. In comparison with other classifiers, outcomes attained reveal that implemented MSVM achieves highest values with a sensitivity of 98.90%, a

Table 2. Simulation results of MSVM by varying the classifiers for the PPMI dataset

Methods	Accuracy (%)	Sensitivity (%)	Specificity (%)	Precision (%)	MCC (%)	F1-score (%)	Recall (%)
Optimized Feature selection results							
NN	91.70	90.55	93.25	92.33	88.71	87.21	85.93
RNN	93.34	94.20	95.66	93.75	93.43	92.47	93.33
GAN	93.30	93.29	90.99	92.48	90.95	91.63	94.58
DNN	91.90	95.0	93.25	94.15	91.65	90.74	92.79
MSVM	98.60	98.90	98.52	98.90	96.87	98.90	99.60
Actual Feature selection results							
NN	89.99	88.55	90.49	89.94	87.53	85.62	84.21
RNN	91.50	89.66	91.86	91.77	90.45	90.35	91.90
GAN	92.98	91.55	94.78	93.85	91.05	89.77	93.12
DNN	94.40	92.75	95.66	95.85	93.21	89.56	90.41
MSVM	96.3	96.6	96.5	96.99	95.53	97.20	97.80

Table 3. PPMI dataset comparison using the IMPA optimization method

Optimized feature selection IMPA optimization method comparison							
Methods	Accuracy (%)	Sensitivity (%)	Specificity (%)	Precision (%)	MCC (%)	F1-score (%)	Recall (%)
EBM	86.98	85.86	87.24	81.60	87.39	88.87	90.98
CNN	84.44	86.76	84.25	84.56	87.20	90.54	92.48
AlexNet	96.33	93.25	94.56	94.92	95.07	91.20	93.81
MLDS	96.15	91.00	96.03	95.14	94.38	94.79	95.30
IMPA	98.60	98.90	98.52	98.90	96.87	98.90	99.60
Actual feature selection IMPA optimization method comparison							
EBM	86.18	85.79	86.25	81.14	87.99	87.10	89.60
CNN	84.17	84.69	85.06	83.59	87.38	89.56	91.48
AlexNet	95.21	93.03	92.14	95.59	91.38	90.99	92.73
MLDS	93.17	90.69	92.89	94.83	95.50	93.61	94.40
IMPA	96.3	96.6	96.5	96.99	95.53	97.20	97.80

Table 4. Performance evaluation of the PPMI dataset's K-fold validation

K-fold values	Sensitivity (%)	Accuracy (%)	Precision (%)	Specificity (%)	MCC (%)	F1-score (%)	Recall (%)
4-fold	94.59	96.09	93.21	94.68	95.71	94.50	95.87
5-fold	98.90	98.60	98.90	98.52	96.87	98.90	99.60
7-fold	93.53	95.89	92.20	94.41	95.35	94.63	94.90
9-fold	93.27	95.46	94.67	93.35	94.54	93.99	95.60
10-fold	92.82	96.57	95.88	92.44	91.96	92.74	96.71

precision of 98.90%, accuracy of 98.60%, a specificity of 98.52%, MCC of 96.87%, F1-score of 98.90%, and recall of 99.60%

Among multi-objective optimization methods used to optimize the IMPA are Explainable Boosting Machine (EBM), Convolutional Neural Network (CNN), AlexNet, Mixture of Linear Dynamical Systems (MLDS) with the selected features obtained on the PPMI dataset. PPMI dataset comparison using the IMPA optimization method is shown in Table 3. When compared to resultant parameters acquired from other optimization methods, the findings of the observation, show that the approach has selected IMPA best set for MSVM to perform at its better phase.

K-fold validation divides dataset into k subsets or folds to evaluate predictive models. Model is trained and estimated k times, employing a various fold serving as validation set every time. Performance metrics from every fold are averaged to evaluate generalization performance of model. This model facilitates model evaluation and selection by giving a more reliable measure of a model's effectiveness. Each fold set training and test would be executed precisely once during this whole process and it assist to prevent overfitting. To achieve k-fold validation, the dataset is divided into three sections: training, testing, and validation. The training and testing datasets are divided into 80:20. When the dataset is into 5 folds and the testing and training processes are done, k=5 results in the model's highest values. Table 4 shows performance evaluation of PPMI dataset's k-fold validation.

4.2 Comparative analysis

In this section, existing and implemented methods' comparative analysis is shown in Table 5. A Machine Learning Detection of PD on DaTSCAN Imagery using Multi-kernel Support Vector Machine as proposed model was determined accurate and has a better classification rate, making them suited for accurately classifying trustworthy, and Parkinson's FImethod of MSVM using PPMI dataset. Compared with other existing methods of EBM [15], LGBM, RF [16], Bayesian CNNs [17], CNN [18], CNN+RLF [22], and EfficientNet-B0, MobileNet-V2 [23] and the implemented method of MSVM using the PPMI

Table 5. Comparative Analysis

Author	Method	Accuracy (%)	Precision	Sensitivity	Specificity	F1-score	Recall
Alessia Sarica [15]	Explainable Boosting Machine (EBM)	88	N/A	N/A	N/A	N/A	N/A
Muhammad Junaid [16]	RF	94	90.39	N/A	N/A	90.06	92.58
Juan E. Arco [17]	Bayesian CNNs	95.31	94.83	94.36	95.76	94.87	N/A
Mahmood Nazari [18]	CNN	96	93	N/A	N/A	94	90
Ankit Kurmi [22]	CNN+FRLF	98.45	98.84	98.84	97.67	98.84	N/A
Hajer Khachnaoui [23]	EfficientNet-B0, MobileNet-V2	98.47	97.51	N/A	N/A	98.51	99.54
Proposed method	MSVM	98.60	98.90	98.90	98.52	98.90	99.60

dataset achieves 98.60% of classification accuracy.

5. Conclusion

The research effectively detects the early Parkinson's disease and builds confidence in use of CAD in medicine. This research implemented the multi-kernel support vector machine for PD detection on DaTSCAN image. This work involves fives steps, which are initially the PPMI datasets were utilized for collecting the PD data. Secondly in pre-processing step, normalization was utilized to ensure that the deep learning model maintained its high degree of performance generalization even after multiple training iterations. Third, feature extraction was done using the VGG-16, and AlexNet to classify Parkinson's illness. Fourth, Improved Marine Predictor Algorithm (IMPA) utilized for feature selection to select the significant features from extracted features. At last, a predicted classification of Parkinson's cases and healthy controls is generated using the MSVM model to improve overall final output of classification method. When compared to existing methods like EBM [15], LGBM, RF [16], Bayesian CNNs [17], CNN [18], CNN+RLF [22], and EfficientNet-B0, MobileNet-V2 [23] the implemented MSVM method achieved high accuracy of 98.60% using PPMI dataset. On the basis on these results, future studies can employ a bigger dataset with the less amount of class imbalance.

Notation

symbol	Description
μ	Mean value
σ	standard deviation
U	uniform distribution
X_i	current solution
lb and ub	lower and upper bounds
r_1 and r_2	uniform random number

m	midpoint of the current search space
$Z1, z2$	dot product of the two vectors
α	Slope
d	intercept constant
Y_t and Y_v	relevant class label sequences
X_t	sequence of images to train
N	number of instances
y_0	negative classes
y_1	positive classes

Conflicts of Interest

The authors declare no conflict of interest.

Author Contributions

The paper conceptualization, methodology, software, validation, formal analysis, investigation, resources, data curation, writing—original draft preparation, have been done by 1st, and 2nd author. The supervision and project administration, writing—review and editing, visualization, have been done by 3rd author.

References

[1] R. Haffar, D. Sanchez, and J. Domingo-Ferrer, "Explaining predictions and attacks in federated learning via random forests", *Applied Intelligence*, Vol. 53, No. 1, pp. 169-185, 2023.

[2] A. Kurmi, S. Biswas, S. Sen, A. Sinitca, D. Kaplun, and R. Sarkar, "An Ensemble of CNN Models for Parkinson's Disease Detection Using DaTscan Images", *Diagnostics*, Vol. 12, No. 5, p. 1173, 2022.

[3] S. S. Aljameel, "A Proactive Explainable Artificial Neural Network Model for the Early Diagnosis of Thyroid Cancer", *Computation*, Vol. 10, No. 10, p. 183, 2022.

[4] N. I. Papandrianos, A. Feleki, S. Moustakidis, E. I. Papageorgiou, I. D. Apostolopoulos, and D. J. Apostolopoulos, "An explainable classification method of SPECT myocardial perfusion images in nuclear cardiology using deep learning and grad-CAM", *Applied Sciences*, Vol. 12, No. 15, p. 7592, 2022.

[5] H. Li, Q. He, and L. Wu, "Detection of Brain Abnormalities in Parkinson's Rats by Combining Deep Learning and Motion Tracking", *IEEE Transactions on Neural Systems and Rehabilitation Engineering*, Vol. 31, pp. 1001-1007, 2023.

[6] C. Adams, J. Suescun, A. Haque, K. Block, S. Chandra, T. M. Ellmore, and M. C. Schiess, "Updated Parkinson's disease motor subtypes classification and correlation to cerebrospinal homovanillic acid and 5-hydroxyindoleacetic acid levels", *Clinical Parkinsonism & Related Disorders*, Vol. 8, p. 100187, 2023.

[7] G. Pezzoli, E. Cereda, P. Amami, S. Colosimo, M. Barichella, G. Sacilotto, A. Zecchinelli, M. Zini, V. Ferri, C. Bolliri, D. Calandrella, M. G. Bonelli, V. Cereda, E. Reali, S. Caronni, E. Cassani, M. Canesi, F. D. Sorbo, P. Soliveri, L. Zecca, C. Klersy, R. Cilia, and I. U. Isaias, "Onset and mortality of Parkinson's disease in relation to type II diabetes", *Journal of Neurology*, Vol. 270, No. 3, pp. 1564-1572, 2023.

[8] M. P. Adams, A. Rahmim, and J. Tang, "Improved motor outcome prediction in Parkinson's disease applying deep learning to DaTscan SPECT images", *Computers in Biology and Medicine*, Vol. 132, p. 104312, 2021.

[9] M. Mozafar, S. Kazemian, E. Hoseini, M. Mohammadi, R. Alimoghadam, M. Shafie, M. Mayeli, and The Parkinson's Progression Markers Initiative, "The glucocerebrosidase mutations and uric acid levels in Parkinson's disease: A 3-years investigation of a potential biomarker", *Clinical Parkinsonism & Related Disorders*, Vol. 8, p. 100177, 2023.

[10] A. Landolfi, M. Picillo, M. T. Pellecchia, J. Troisi, M. Amboni, P. Barone, and R. Erro, "Screening performances of an 8-item UPSIT Italian version in the diagnosis of Parkinson's disease", *Neurological Sciences*, Vol. 44, No. 3, pp. 889-895, 2023.

[11] M. Martinez-Eguiluz, O. Arbelaitz, I. Gurrutxaga, J. Muguerza, I. Perona, A. Murueta-Goyena, M. Acera, R. D. Pino, B. Tijero, J. C. Gomez-Esteban, and I. Gabilondo, "Diagnostic classification of Parkinson's disease based on non-motor manifestations and machine learning strategies", *Neural Computing and Applications*, Vol. 35, No. 8, pp. 5603-5617, 2023.

[12] E. A. Katunina, V. Blokhin, M. R. Nodel, E. N. Pavlova, A. L. Kalinkin, V. G. Kucheryanu, L. Alekperova, M. V. Selikhova, M. Y. Martynov, and M. V. Ugrumov, "Searching for Biomarkers in the Blood of Patients at Risk of Developing Parkinson's Disease at the Prodromal Stage", *International Journal of Molecular Sciences*, Vol. 24, No. 3, p. 1842, 2023.

[13] J. Hathaliya, R. Parekh, N. Patel, R. Gupta, S. Tanwar, F. Alqahtani, M. Elghatwary, O. Ivanov, M. S. Raboaca, and B.-C. Neagu, "Convolutional neural network-based Parkinson disease classification using SPECT imaging data", *Mathematics*, Vol. 10, No. 15, p. 2566, 2022.

[14] D. Z. Milikovsky, Y. Sharabi, N. Giladi, A. Mirelman, R. Sosnik, F. Fahoum, and I. Maidan, "Paroxysmal Slow-Wave Events Are Uncommon in Parkinson's Disease", *Sensors*, Vol. 23, No. 2, p. 918, 2023.

[15] A. Sarica, A. Quattrone, and A. Quattrone, "Explainable machine learning with pairwise interactions for the classification of Parkinson's disease and SWEDD from clinical and imaging features", *Brain Imaging and Behavior*, Vol. 16, No. 5, pp. 2188-2198, 2022.

[16] M. Junaid, S. Ali, F. Eid, S. El-Sappagh, and T. Abuhmed, "Explainable machine learning models based on multimodal time-series data for the early detection of Parkinson's disease", *Computer Methods and Programs in Biomedicine*, Vol. 234, p. 107495, 2023.

[17] J.E. Arco, A. Ortiz, J. Ramírez, F. J. Martínez-Murcia, Y.-D. Zhang, and J. M. Górriz, "Uncertainty-driven ensembles of multi-scale deep architectures for image classification", *Information Fusion*, Vol. 89, pp. 53-65, 2023.

[18] M. Nazari, A. Kluge, I. Apostolova, S. Klutmann, S. Kimiaei, M. Schroeder, and R. Buchert, "Explainable AI to improve acceptance of convolutional neural networks for automatic classification of dopamine transporter SPECT in the diagnosis of clinically uncertain parkinsonian syndromes", *European Journal of Nuclear Medicine and Molecular Imaging*, Vol. 49, No. 4, pp. 1176-1186, 2022.

[19] K. Nakajima, S. Saito, Z. Chen, J. Komatsu, K. Maruyama, N. Shirasaki, S. Watanabe, A. Inaki, K. Ono, and S. Kinuya, "Diagnosis of Parkinson syndrome and Lewy-body disease using 123I-ioflupane images and a model with image

features based on machine learning", *Annals of Nuclear Medicine*, Vol. 36, No. 8, pp. 765-776, 2022.

[20] N. Alsharabi, T. Shahwar, A. U. Rehman, and Y. Alharbi, "Implementing Magnetic Resonance Imaging Brain Disorder Classification via AlexNet–Quantum Learning", *Mathematics*, Vol. 11, No. 2, p. 376, 2023.

[21] Y. Zhou, S. Tinaz, and H. D. Tagare, "Robust Bayesian Analysis of Early-Stage Parkinson's Disease Progression Using DaTscan Images", *IEEE Transactions on Medical Imaging*, Vol. 40, No. 2, pp. 549-561, 2021.

[22] A. Kurmi, S. Biswas, S. Sen, A. Sinitca, D. Kaplun, and R. Sarkar, "An ensemble of CNN models for Parkinson's disease detection using DaTscan images", *Diagnostics*, Vol. 12, No. 5, p.1173, 2022.

[23] H. Khachnaoui, B. Chikhaoui, N. Khlifa, and R. Mabrouk, "Enhanced Parkinson's Disease Diagnosis Through Convolutional Neural Network Models Applied to SPECT DaTSCAN Images", *IEEE Access,* Vol. 11, pp. 91157-91172 2023.